Metabolism Clinical and Experimental 88 (2018) 22–30

Contents lists available at ScienceDirect

Metabolism Clinical and Experimental

journal homepage: www.metabolismjournal.com

cGMP-dependent protein kinase I (cGKI) modulates human hepatic stellate cell activation

Andras Franko [a,b,c], Marketa Kovarova [a,b,c], Susanne Feil [d], Robert Feil [d], Robert Wagner [a,b,c], Martin Heni [a,b,c], Alfred Königsrainer [e], Marc Ruoß [f], Andreas K. Nüssler [f], Cora Weigert [a,b,c], Hans-Ulrich Häring [a,b,c], Stefan Z. Lutz [a,b,c,*], Andreas Peter [a,b,c]

[a] Department of Internal Medicine IV, Division of Endocrinology, Diabetology, Angiology, Nephrology and Clinical Chemistry, University Hospital Tübingen, Otfried-Müller-Str 10, 72076 Tübingen, Germany
[b] Institute for Diabetes Research and Metabolic Diseases, Helmholtz Center Munich, University of Tübingen, Otfried-Müller-Str 10, 72076 Tübingen, Germany
[c] German Center for Diabetes Research (DZD e.V.), Ingolstädter Landstraße 1, 85764 Neuherberg, Germany
[d] Interfakultäres Institut für Biochemie, University of Tübingen, Hoppe-Seyler-Str. 4, 72076 Tübingen, Germany
[e] Department of General, Visceral and Transplant Surgery, University Hospital Tübingen, Hoppe-Seyler-Straße 3, 72076 Tübingen, Germany
[f] Department of Traumatology, BG Trauma Clinic, Siegfried Weller Institute for Trauma Research, Eberhard Karls Universität Tübingen, Schnarrenbergstr. 95, 72076 Tübingen, Germany

ARTICLE INFO

Article history:
Received 6 June 2018
Accepted 3 September 2018

Keywords:
cGKI
Hepatic stellate cell
Inflammation
Insulin resistance
Liver
LX2 cell

ABSTRACT

Background: The activation of hepatic stellate cells (HSCs) plays a crucial role in liver fibrosis, however the role of HSCs is less understood in hepatic insulin resistance. Since in the liver cGMP-dependent protein kinase I (cGKI) was detected in HSC but not in hepatocytes, and cGKI-deficient mice that express cGKI selectively in smooth muscle but not in other cell types (cGKI-SM mice) displayed hepatic insulin resistance, we hypothesized that cGKI modulates HSC activation and insulin sensitivity.
Materials and Methods: To study stellate cell activation in cGKI-SM mice, retinol storage and gene expression were studied. Moreover, in the human stellate cell line LX2, the consequences of cGKI-silencing on gene expression were investigated. Finally, cGKI expression was examined in human liver biopsies covering a wide range of liver fat content.
Results: Retinyl-ester concentrations in the liver of cGKI-SM mice were lower compared to wild-type animals, which was associated with disturbed expression of genes involved in retinol metabolism and inflammation. cGKI-silenced LX2 cells showed an mRNA expression profile of stellate cell activation, altered matrix degradation and activated chemokine expression. On the other hand, activation of LX2 cells suppressed cGKI expression. In accordance with this finding, in human liver biopsies, we observed a negative correlation between cGKI mRNA and liver fat content.
Conclusions: These results suggest that the lack of cGKI possibly leads to stellate cell activation, which stimulates chemokine expression and activates inflammatory processes, which could disturb hepatic insulin sensitivity.

1. Introduction

Hepatic inflammation is strongly associated with insulin resistance [1], and it can progress to non-alcoholic steatohepatitis (NASH), hepatic fibrosis and cirrhosis [2]. Hepatic stellate cells (HSCs) are located in the space of Disse adjacent to hepatocytes, Kupffer cells and endothelial cells (ECs) and play a central role in liver fibrogenesis [3]. Under quiescent conditions, HSCs contain most of the body's Vitamin A (retinol) as retinyl-esters [4]. Upon activation, they lose the stored retinyl-esters, express extracellular matrix proteins (ECMs) like collagen as well as matrix remodeling enzymes like matrix metallopeptidases (MMPs) and tissue inhibitor of metallopeptidases (TIMPs) [5]. Activated HSCs are key drivers of liver fibrosis/cirrhosis via ECM production [6] and they could also stimulate oncogenic pathways [7]. Recent studies showed, that in addition to fibrogenesis, HSCs play a central role in inflammatory processes expressing inflammatory cytokines [8]. Furthermore, HSCs were demonstrated to be involved in the chemotactic recruitment of Kupffer cells, monocytes and macrophages

Abbreviations: α-SMA, alpha smooth muscle actin; cGKI, cGMP-dependent protein kinase I; cGKI-SM, cGKI-smooth muscle rescue mice; ECM, extracellular matrix; HSC, hepatic stellate cell; IPA, Ingenuity Pathway Analysis; MMP, matrix metallopeptidase; NAFLD, non-alcoholic fatty liver disease; NASH, non-alcoholic steatohepatitis; RP, retinyl-palmitate; PHH, primary human hepatocyte; TAG, triacylglycerol; TIMP, tissue inhibitor of metallopeptidase; TGFβ, transforming growth factor beta.

* Corresponding author at: Department of Internal Medicine IV, Division of Endocrinology, Diabetology, Angiology, Nephrology and Clinical Chemistry, University Hospital Tübingen, Otfried-Müller-Str. 10, 72076 Tübingen, Germany.
E-mail address: stefan.lutz@med.uni-tuebingen.de (S.Z. Lutz).

https://doi.org/10.1016/j.metabol.2018.09.001

from the circulation into the injured liver area through chemokine production [3]. The pathways triggering HSC activation, in particular in non-alcoholic fatty liver disease (NAFLD) and insulin resistance are less clear. In our previous study, we have found that mice expressing cGMP-dependent protein kinase I (cGKI) selectively in smooth muscle but not in other cell types (cGKI-SM mice) exhibit hepatic macrophage infiltration, which was postulated to elevate hepatic inflammation and in turn led to insulin resistance [9]. Nitric oxide (NO) elevates cGMP levels, which activates cGKI [10]. NO signaling was also shown to regulate intrahepatic vascular resistance, which is a characteristic property of NAFLD [11]. Furthermore, insulin resistance is associated with endothelial dysfunction in young relatives of patients with type 2 diabetes (T2D) suggesting a dysregulated NO signaling in patients with high liver fat [12]. In the liver, immunostaining for cGKI was positive in stellate cells but not in hepatocytes [9] suggesting that cGKI has a stellate cell specific function. To prove the hypothesis that the lack of cGKI triggers HSC activation leading to hepatic inflammation and insulin resistance, in this study the retinyl-ester storage and expression of genes involved in retinol metabolism and inflammation were studied in liver of cGKI-SM mice. To investigate stellate cell metabolism, we used the human hepatic stellate cell line LX2, which has been previously validated as a suitable model expressing activation markers like alpha smooth muscle actin (α-SMA), MMPs and TIMPs [13]. To explore the key metabolic pathways disturbed by the ablation of cGKI, we investigated the consequences of silencing cGKI by siRNA. Furthermore, we studied cGKI mRNA expression in human liver biopsies covering a broad range of liver fat content.

2. Materials and Methods

2.1. Materials

Chemicals were purchased from Sigma-Aldrich (Germany) unless stated otherwise.

2.2. Animal Studies

Male and female mice that express cGKI selectively in smooth muscle but not in other cell types (cGKI-SM mice [9]) were analyzed at two–three months of age as described previously [9,14]. Liver triacylglycerol (TAG) and retinoid levels were measured as described previously [15,16]. Total liver RNA was isolated from liver tissues using RNeasy Mini Kit (Qiagen, Germany) with MagNA Lyser Green Beads (Roche, Germany) according to the manufacturer's description. All animals received humane care and mouse studies were approved by local government authorities and performed according to GV-SOLAS (Society for Laboratory Animal Science) in accordance with the German Animal Welfare Act.

2.3. Microarrays

RNA integrity was determined with the Agilent 2100 Bioanalyzer and Eukaryote Total RNA Nano Kit (Agilent Technologies, Germany). cDNA synthesis and hybridization to Affymetrix GeneChip Mouse Gene 2.0 ST arrays (Affymetrix, Inc., Germany) were conducted as described by the manufacturer's specifications. Array images were analyzed using Affymetrix Expression Console 1.4.1 software. Signal intensities were log-transformed and normalization was performed by RMA (robust multi-array average) method. Array data were submitted to the NCBI GEO database at NCBI (GSE111988). Statistical analysis was performed in MultiExperiment Viewer (MeV, version 4.9.0) using the Significance Analysis of Microarrays algorithm with 1000 permutations and a local false discovery rate (FDR) of <10% [17]. Pathway analysis was performed with Ingenuity Pathway Analysis (IPA) tool (Qiagen).

2.4. Cell Culture

Primary human hepatocytes (PHH) were isolated by a two-step EDTA/collagenase perfusion technique as described previously with the following modifications: To stop the collagenase digestion, a solution with 20% FBS in phosphate-buffered saline (PBS) was used. To minimize proteolytic enzyme activities, the collagenase solution was mixed 1:1 with the perfusion solution II. Hepatocytes were cultivated for one day in Williams Medium E containing 10% FBS [18]. Indications for the surgery were hepatic hemangioma, curative resection of hepatic metastases of colorectal malignancies or hepatocellular carcinoma. Liver samples were taken from normal, non-diseased tissue during surgery. Informed, written consent was obtained from all participants, and the Ethics Committee of the University of Tübingen approved the protocol according to the Declaration of Helsinki.

The human immortalized hepatic stellate cell line LX2 cells (Millipore, Germany, #SCC064) were kept at humidified atmosphere (at 5% CO_2, 37 °C) and cultured in 2% FBS containing DMEM media (Gibco, Germany) supplemented with penicillin/streptomycin. For experiments, LX2 cells were seeded on the first day on 6-well plates and transfected on the second day with ON-TARGETplus Human *PRKG1* (5592) siRNA SMARTpool (Dharmacon, Germany, #L-004658-00-0005) or with ON-TARGETplus Non-targeting pool siRNA (Dharmacon, #D-001810-10-20) using Viromer Blue (Lypocalyx, Germany, #VB-01LB-01) according to the manufacturer's description. On the third and fourth days, LX2 cells were treated with human TGFβ1 (R&D Systems, Germany, #100-B-001) at the given concentrations and cells were harvested on the fifth day. To keep LX2 cells quiescent for the indicated experiments, cells were treated with 10 μM retinol, 100 μM BSA-coupled palmitate, 500 μM isobutylmethylxanthine (IBMX), 1 μM dexamethasone, and 167 nM insulin (MDI) as it was published previously [19,20]. Biological replicates represent three–four independent experiments.

2.5. Human Liver Biopsies

In addition, data for the analysis of liver tissue samples, a cohort of 105 European descendent men and women (37 women/68 men, age 63 ± 12 years, weight 76 ± 13 kg, BMI 25.2 ± 4.1 kg/m^2) undergoing liver surgery at the Department of General, Visceral, and Transplant Surgery at the University Hospital of Tübingen was included in the present study. Indications for the surgery were hepatic hemangioma, curative resection of hepatic metastases of colorectal malignancies or hepatocellular carcinoma. Liver samples were taken from normal, non-diseased tissue during surgery. Patients were fasted overnight before collection of liver biopsies. Subjects were tested negative for viral hepatitis and had no liver cirrhosis. Informed, written consent was obtained from all participants, and the Ethics Committee of the University of Tübingen approved the protocol (239/2013BO1) according to the Declaration of Helsinki. Liver samples were immediately frozen in liquid nitrogen, and stored at −80 °C. Liver tissue samples were homogenized in PBS containing 1% Triton X-100 with a TissueLyser (Qiagen). To determine the liver fat content, TAG concentrations in the homogenate were quantified using an ADVIA XPT clinical chemistry analyzer (Siemens Healthineers, Germany), and the results were calculated as mg/100 mg tissue weight (%) as described previously [21]. For RNA isolation frozen tissue was homogenized in a TissueLyser (Qiagen) and total RNA was isolated as described below.

2.6. Real-Time PCR

Total RNA from LX2 cells or from human liver biopsies were isolated with Allprep RNA/DNA/protein kit (Qiagen) or with RNeasy Mini Kit (Qiagen), respectively according to the manufacturer's description and 500 ng total RNA was applied for cDNA synthesis (Transcriptor First Strand cDNA synthesis kit, Roche). Real-time PCRs were performed with LightCycler 480 Probes Master (Roche) with universal probe

library (primer sequences and probe numbers are listed in Supplementary Tables 1 and 2) using LightCycler 480 (Roche) as published previously [15]. Delta-delta crossing-point (Cp) values were calculated and values were normalized to the geometric mean of the housekeeping genes ribosomal protein S13 (*Rps13*) and ubiquitin c (*UBC*) for LX2 cells. Three–four independent experiments of LX2 cells were normalized to experimental averages, and then to untreated controls (shown as one).

2.7. Western Blot

Proteins were isolated with Allprep RNA/DNA/protein kit (Qiagen) or with RIPA buffer supplemented with proteinase and phosphatase inhibitors [22]. Seven to fifteen micrograms of proteins was loaded on 10% acrylamide gel and blotted onto a nitrocellulose membrane (GE Healthcare, Germany). After 1 h saturation in NETG [22] the antigen was labeled with the appropriate first antibody (cGKI: Cell Signaling, #3248; α-SMA: Cell Signaling, #1945; albumin: Santa Cruz, #sc-271605; TIMP2: Biotechne/R&D systems, #AF971; GAPDH: Abcam, #8245, Germany) in NETG for overnight. After washing with NETG, the appropriate secondary antibodies (anti-rabbit HRP, anti-mouse HRP, anti-goat HRP; Santa Cruz, TX, USA) were used in NETG and after final washing the blot was developed with enhanced chemiluminescence using ChemiDoc Touch Imaging System (BioRad, Germany). Protein bands were evaluated by densitometry and data for three–four independent experiments were normalized to loading controls, then to experimental averages, and finally to untreated controls (shown as one).

2.8. NFkB Promoter Activity

LX2 cells were cultured in 2% FBS and transfected with NFkB promoter-Firefly vector (Clonetech/Takara, USA) and pRL-CMV-Renilla control vector (Promega, USA) in the absence or presence of negative siRNA or cGKI siRNA using Viromer Red (Lypocalyx, Germany). Luciferase assay was measured 46 h after transfection using GloMax Multidetection System Luminometer (Promega) as described previously [23]. Values were normalized to untransfected controls and NFkB promoter driven Firefly values were divided by the constitutive cytomegalovirus (CMV) promoter driven values. Finally, data were normalized to plasmid DNA transfected conditions without siRNA (shown as one).

2.9. Statistics

Statistical evaluations were performed using GraphPad Prism 7.03. To compare cGKI-SM with control mice, Students *t*-tests were performed. To calculate statistical significance for LX2 cells in five different conditions, ANOVA with post hoc Holm-Šídák's multiple comparison tests were used. Statistical significance was assumed as $p < 0.05$, unless otherwise stated.

3. Results

3.1. cGKI is Expressed in Stellate Cells but not in Hepatocytes

Our previous histological investigations in mice suggested that cGMP-dependent protein kinase I (cGKI) expression in the liver is only detectable in stellate cells, but not in hepatocytes [9]. To verify this observation in humans and to validate our cell culture model, we compared primary human hepatocytes (PHH) with the human stellate cell line LX2. As expected, LX2 cells expressed the myofibroblast specific protein α-smooth muscle actin (α-SMA) (Fig. 1A, upper panel) suggesting that this cell line is partly activated as it was published previously [13]. PHH did not express α-SMA (Fig. 1A, upper panel) but albumin was detected in these cells (Fig. 1A, middle panel). cGKI antibody recognized a prominent band in LX2 cells, however PHH did not show any signal for this antibody (Fig. 1A, lower panel) indicating that cGKI is stellate cell specific.

3.2. cGKI-SM Mice Show Signs for Stellate Cell Activation

Since our previous study demonstrated that ablation of cGKI resulted in elevated hepatic inflammation and insulin resistance, which might be a consequence of stellate cell activation [9] we analyzed the livers of these animals in more detail. In accordance with previous data, the hepatic triacylglycerol (TAG) level of cGKI-SM mice was lower compared to control mice (Supplementary Fig. 1A). We next performed a transcriptomics analysis of the global hepatic gene expression in these animals. Significance analysis of microarray (SAM) analysis revealed 55 genes, which were significantly changed in cGKI-SM mice compared to controls (Supplementary Table 3). The most prominent genes are shown in Fig. 1B. Many genes, which are involved in inflammatory processes and iron metabolism, were significantly upregulated in cGKI-SM mice (Fig. 1B). Genes responsible for lipid and retinol metabolism showed a significant downregulation, however genes coding for extracellular matrix proteins were upregulated in cGKI-SM mice (Fig. 1B). Selected significantly regulated genes in the microarray were verified by quantitative real-time PCR (Fig. 1C). In order to investigate, which pathways are changed in the liver of cGKI-SM mice, the significantly regulated genes were analyzed using the Ingenuity Pathway Analysis (IPA) tool. IPA could not only detect significantly enriched pathways using *p*-values (significance is assumed as $p < 0.1000$), but is also able to identify, whether the pathway is significantly upregulated by z-scores (z-score > 2). To determine the consequences of the ablation of cGKI in the liver, different IPA pathways including the Toxicity list, Upstream regulators and Canonical pathways were analyzed. Among the Canonical pathways, the retinol biosynthesis pathway was significantly enriched (p-value = 0.0490). IPA showed that pathways responsible for cytochrome P450, oxidative stress, liver necrosis, fatty acid metabolism and acute phase response protein pathways (Table 1, Toxicity list) were significantly enriched. Furthermore, IPA demonstrated a significant enrichment of upstream regulators of inflammatory pathways and stellate cells activators (Table 1, Upstream Regulators list, *p*-values), which were upregulated significantly (z-score > 2) or by trend (z-score 1 < 2) (Table 1, Upstream Regulators list, z-scores). To study the stored Vitamin A content in the liver of cGKI-SM mice, we measured hepatic retinol and retinyl-ester content. cGKI-SM mice showed significantly lower concentrations of all studied retinyl-esters compared to control mice (Fig. 1D). The reduced retinyl-ester storage and the upregulated inflammatory (interleukin 1, 6 and tumor necrosis factor) and stellate cell activator (platelet-derived growth factor B) pathways suggest that the absence of cGKI evokes an activation of hepatic stellate cells in cGKI-SM mice.

3.3. cGKI Level Decreases During Activation of Stellate Cells

In order to study whether the absence of cGKI directly impacts on stellate cell activation, we used the human hepatic stellate cell line LX2. Since quiescent stellate cells store retinyl-esters, we have first measured intracellular retinyl-palmitate (RP) levels in LX2 cells. To induce intracellular RP storage, LX2 cells were treated with retinol and palmitate. Furthermore, we applied a treatment protocol that has been shown to induce a quiescent state in stellate cells containing isobutylmethylxanthine (IBMX), dexamethasone, and insulin (MDI) [19] in combination with retinol and palmitate. Intracellular RP was detected in LX2 cells treated with retinol and palmitate in the presence or absence of MDI (quiet1 and quiet2 conditions, Fig. 2A), however untreated cells did not store RP (basal condition, Fig. 2A). Furthermore, retinol and palmitate supplementation was essential for RP storage in LX2 cells, since withdrawal of retinol and palmitate for one day led to depletion of RP stores ("-ret + pal" condition, Fig. 2A). Since high serum concentrations are known to activate stellate cells [20], the normal 2% FBS (used routinely for culture conditions keeping cells rather in inactivated state) was exchanged to 10% FBS. As expected, LX2 cells showed a trend to lower RP stores when cultured in 10% FBS (activated condition, Fig. 2A) suggesting that LX2 cells are partly activated under

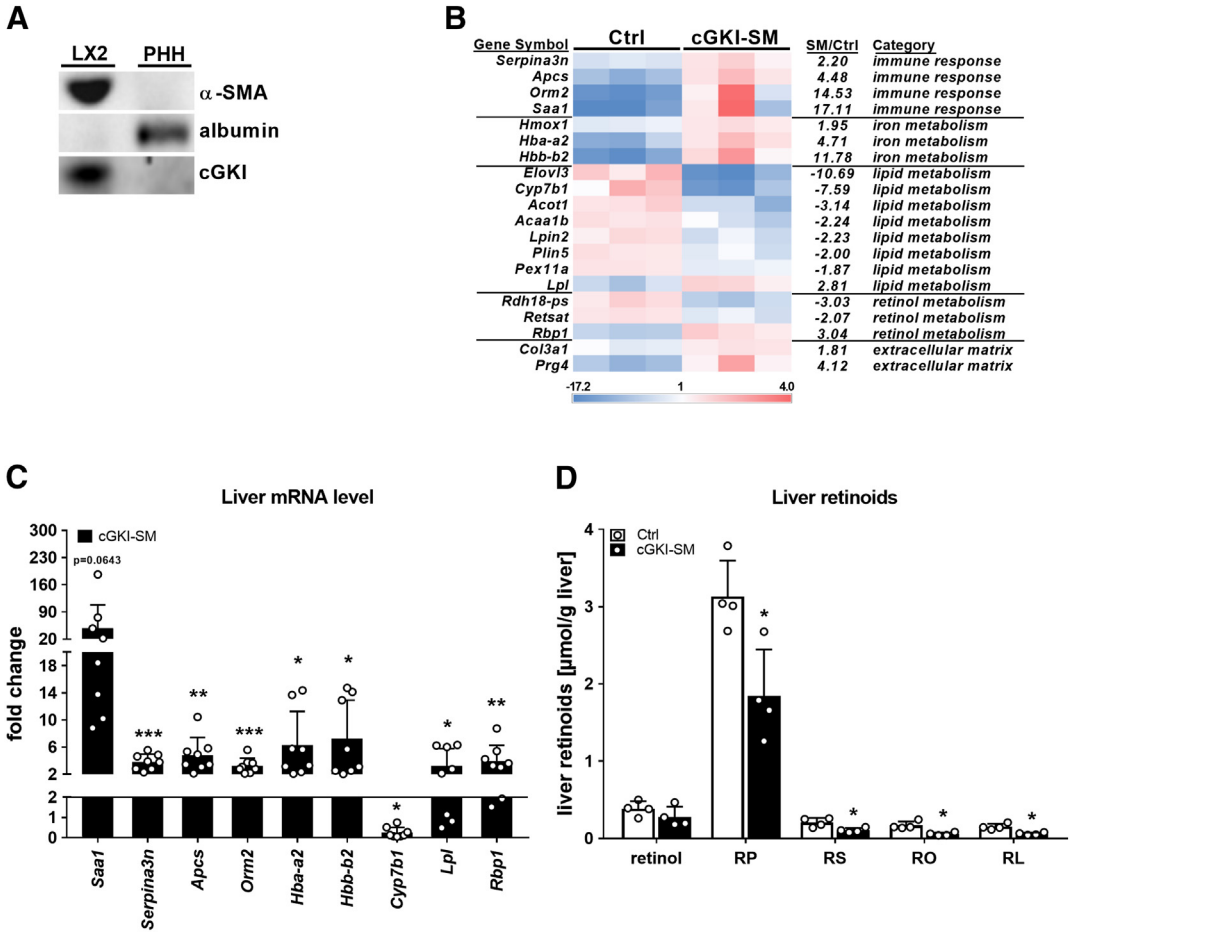

Fig. 1. cGKI is expressed in stellate cells and cGKI-SM mice show signs for stellate cell activation. *A*: The intracellular protein composition of primary human hepatocytes (PHH) was compared to human stellate cell line LX2 using Western blot with the indicated antibodies. *B*: Important, differently expressed hepatic genes were chosen from microarray analysis of cGKI-SM and control (Ctrl) mice shown as a heat map. Red color indicates upregulated genes, blue color indicates downregulated genes normalized to group averages (set as one). The complete gene names are given in Suppl. Table 3. SM/Ctrl ratios indicate the group averages of cGKI-SM mice divided by the averages of control animals. Genes, which showed lower expression in cGKI-SM mice, are shown as inverted ratios with minus; n:3. *C*: mRNA levels of hepatic genes were determined by real-time PCR from liver samples of cGKI-SM and control mice. Values were normalized to the housekeeping gene *RPS13*; n:8–10. Number denotes *p*-value calculated by Students *t*-test. *D*: Hepatic retinoid levels of cGKI-SM and control mice measured by high-performance liquid chromatography. RP: retinyl-palmitate, RS: retinyl-stearate, RO: retinyl-oleate, RL: retinyl-linoleate; n:4. Columns represent averages ± standard deviations; * denotes significant differences between cGKI-SM and control mice; $^{*}p < 0.05$, $^{**}p < 0.01$, $^{***}p < 0.001$.

these conditions. To further mimic stellate cell activation in vitro, LX2 cells were activated with 10% FBS for two days in the presence of transforming growth factor beta (TGFβ), a cytokine, which is known to induce stellate cell activation [20] and liver fibrosis [6]. The gene expression profile of key markers for stellate cell activation was studied using real-time PCR. Increasing concentration of TGFβ led to elevated transcript levels of alpha smooth muscle actin (*α-SMA*), collagen type I alpha 1 chain (*COL1A1*), transforming growth factor beta induced (*TGFβi*), connective tissue growth factor (*CTGF*), matrix metallopeptidase 2 (*MMP2*) and tissue inhibitor of metallopeptidase 2 (*TIMP2*) in LX2 cells (Fig. 2B–G). TGFβ treatment decreased the mRNA expression of peroxisome proliferator activated receptor gamma (*PPARγ*) (Fig. 2H), which is a marker of quiescent stellate cells [3]. Since elevated expressions of *α-SMA*, *COL1A1*, *CTGF*, *MMP2* and *TIMP2* are characteristic for activated stellate cells [5], these results suggest that 10% FBS in the presence of TGFβ resulted in the activation of LX2 cells. Interestingly, the transcript as well as protein levels of cGKI were reduced upon stimulation (Fig. 2I–J) strongly indicating that activation of stellate cells suppresses cGKI expression. Since quiescent stellate cells could be different from non-quiescent cells, we also analyzed LX2 cells, which were kept in quiescent condition for one day with retinol, palmitate and MDI and got activated on the consecutive day. As shown for the non-quiescent LX2 cells (Fig. 2), the transcripts of *α-SMA*, *TGFβi* and *MMP2* were also upregulated in quiescent LX2 cells upon the TGFβ stimulus (Supplementary Fig. 1B–D). Furthermore, the transcript of cGKI was reduced during the activation of quiescent LX2 cells (Supplementary Fig. 1E).

3.4. The Ablation of cGKI Results in Elevated Activation of Stellate Cells

After establishing the appropriate conditions for in vitro stellate cell activation, LX2 cells were transfected with cGKI specific siRNA to reduce intracellular cGKI levels. Real-time PCR and Western blot experiments showed that cGKI levels are significantly reduced in cGKI siRNA treated cells compared to negative siRNA controls (Fig. 3A–B). Silencing cGKI significantly increased the transcripts of *α-SMA* and *TGFβi* in the presence of TGFβ, and it elevated the transcript of *MMP2* in all studied conditions (Fig. 3C–E). The transcript levels of *TIMP2* and *PPARγ* were significantly reduced upon silencing cGKI (Fig. 3F–G). The higher transcript levels of *α-SMA* and *MMP2* and the lower *TIMP2* level in cGKI siRNA knock-down cells were also verified in quiescent LX2 cells in the presence (Supplementary Fig. 1F–I) or absence of fetal bovine serum (FBS) (Supplementary Fig. 1J). The higher level of α-SMA and the lower level of TIMP2 upon cGKI siRNA knock-down were verified at protein level, however the observed changes remained non-

Table 1
Significantly enriched pathways of hepatic genes.

Ingenuity toxicity lists			*p*-value
Cytochrome P450 panel - substrate is a fatty acid (mouse)			0.0525
Increases damage of mitochondria			0.0525
NRF2-mediated oxidative stress response			0.0490
Liver necrosis/cell death			0.0191
Fatty acid metabolism			0.0138
Positive acute phase response proteins			<0.0001
Ingenuity upstream regulators	**Name**	**z-score**	***p*-value**
NFκB complex	Nuclear factor kappa-light-chain-enhancer of activated B cells	1.01	<0.0001
STAT3	Signal transducer and activator of transcription 3	1.75	0.0009
TNF	Tumor necrosis factor	1.81	<0.0001
IL1B	Interleukin 1 beta	1.96	<0.0001
IL1A	Interleukin 1 alpha	1.96	0.0010
IL6	Interleukin 6	1.98	<0.0001
NOS2	Nitric oxide synthase, inducible	**2.19**	<0.0001
PDGF BB	Platelet-derived growth factor beta	**2.22**	0.0004

Hepatic gene expression was analyzed using microarray and Significance Analysis of Microarrays (SAM) algorithm was applied with False Discovery Rate (FDR) less than <10%, which identified 55 differently expressed genes comparing cGKI-SM mice to controls. These 55 genes were analyzed by Ingenuity Pathway Analysis (IPA), which identified significantly enriched pathways, some of them are shown as Table 1. *p*-values represent Benjamini-Hochberg corrected *p*-values, positive z-scores represent that the pathways are upregulated, z-scores>2 indicate significantly upregulated pathways. Significance for pathway enrichment is shown as *p*-values, which was assumed as $p < 0.1000$.

significant (Supplementary Fig. 1K–L). Since patatin-like phospholipase domain-containing protein 3 (PNPLA3) was recently shown to contribute to stellate cell activation [20], we also analyzed the transcript level of PNPLA3. Silencing cGKI significantly elevated the expression of *PNPLA3* (Fig. 3H). These results indicate that independently of the basal activation state, the lack of cGKI promotes the expression of key stellate cell genes leading to activation of LX2 cells. In order to study the role of cGKI in retinyl-palmitate storage, LX2 cells were transfected with cGKI siRNA and RP levels were measured. Silencing of cGKI did not influence the stored RP levels in LX2 cells in any of the analyzed conditions (Fig. 3I).

Since activated stellate cells could recruit macrophages, granulocytes and monocytes to the location of liver injury via elevated chemokine secretion [3], we analyzed the transcripts of known chemokines involved in this process. Silencing cGKI significantly elevated the transcript levels of interleukin 8 (*IL8*), chemokine (C-C motif) ligand 5 (*CCL5*) and chemokine (C-X-C motif) ligand 1 (*CXCL1*) chemokines as well as the level of toll-like receptor 4 (*TLR4*), which is a known marker for activated stellate cells [4] (Fig. 4A–D). Since TGFβ was shown to mediate both pro and anti-inflammatory effects [24], it is not unexpected that TGFβ treatment led to decreased chemokine secretion, as it was also shown for LX2 cells [25]. In order to investigate key factors, which could regulate chemokine expression, we measured nuclear factor kappa-light-chain-enhancer of activated B cells (NFkB) promoter activity using luciferase assay. The knock-down of cGKI increased NFkB promoter activity compared to negative siRNA condition (Fig. 4E). Our results suggest that the absence of cGKI leads not only to activation of LX2 cells but also to elevated chemokine secretion, which could be regulated by NFkB.

3.5. cGKI mRNA Levels in Human Liver Biopsies Are Negatively Associated With Liver Fat

Finally, we tested the relevance of cGKI in human fatty liver disease and analyzed the transcript expression of *cGKI* in human liver biopsies covering a wide range of liver fat content. In these human samples *cGKI* mRNA expression was negatively correlated with liver fat content (Fig. 4F) suggesting that hepatic cGKI is downregulated during accumulation of liver fat.

4. Discussion

cGKI-SM mice display a striking liver phenotype of hepatic macrophage infiltration, inflammation and insulin resistance [9], which is only poorly understood. We hypothesized that in cGKI-SM mice, hepatic insulin resistance is induced by HSC activation triggered by the lack of cGKI, which induces macrophage infiltration and hepatic inflammation. In the present study we detected low hepatic retinyl-ester storage in cGKI-SM mice, which is characteristic for stellate cell activation. This was accompanied by a hepatic transcript profile, which was enriched in genes involved in retinol metabolism and upregulated pathways known to activate HSCs (like PDGF) [3]. The upregulated inflammatory modulators identified by the IPA analysis in cGKI-SM mice mostly belong to the pro-inflammatory pathways (TNF, IL1, IL6). Since IL1 and TNFα have been already shown to be involved in HSC and macrophage crosstalk [26] they could at least in part mediate the effects of cGKI in stellate cell activation.

Taken together, our data from the liver of cGKI-SM mice and from the cGKI siRNA knock-down human hepatic stellate cell line LX2 cells suggest that at least three major stellate cell functions are modulated by cGKI (Fig. 4G). The ablation of cGKI results in activation of stellate cells (Function 1), altered ECM remodeling (Function 2) and elevated chemokine secretion (Function 3).

Function 1: The lack of cGKI increased the transcript of *α-SMA* and suppressed the mRNA of *PPARγ*. α-SMA is a characteristic marker for activated HSCs [27] and cGKI activation with sildenafil was shown to decrease α-SMA level in the kidney [28]. PPARγ is a quiescent HSC marker and it is needed to be silenced at transcriptional level for the conversion of quiescent HSC to myofibroblast [29]. Therefore our results suggest that via the regulation of α-SMA and PPARγ, the absence of cGKI induces a possible transdifferentiation of quiescent stellate cells to myofibroblasts in LX2 cells.

Function 2: The ablation of cGKI elevated the mRNA of *MMP2* and decreased the transcript of *TIMP2*. During stellate cell activation, cells secrete a high amount of ECM proteins in association with elevated levels of MMPs, which are involved in the digestion and remodeling of ECM proteins [5]. TIMPs are specific inhibitors of MMPs but TIMP2 has also the capacity to activate MMP2 [30]. TIMPs are also expressed on higher levels during liver fibrosis and stellate cell activation [31], and a high MMP/TIMP ratio is a typical hallmark of activated state [5]. Since the ablation of cGKI elevated MMP2/TIMP2 ratio, these results implicate that cGKI may alter matrix remodeling activity in LX2 cells.

Function 3: The absence of cGKI increased the transcript levels of *TLR4*, *IL8*, *CCL5* and *CXCL1*. Activated HSCs express TLR2, TLR3, TLR4, TLR7 and TLR9, from which TLR4 was shown to upregulate chemokine secretion, to induce chemotaxis of macrophages and to be involved in ROS signaling [3,26]. Therefore, it is possible that the higher TLR4 level in cGKI silenced LX2 cells is also involved in the induction of chemokines. In the liver, HSCs were shown to secrete CXCL1, which is responsible for the recruitment of neutrophil granulocytes [32]. CCL5 is a chemokine, which recruits monocytes to the liver [26]. Blocking CCL5 with receptor antagonist resulted in decreased HSC migration and proliferation in mice and LX2 cells, respectively [3,33]. IL8 is a chemokine, which recruits and activates leukocytes during inflammation and it was shown to be responsible for the induction of α-SMA from LX2 cells co-cultured with human hepatoma cells transfected with HCV protein [34]. Furthermore, the cGKI-SM mice showed signs of macrophage infiltration in the liver [9]. Thus, the higher chemokine expression of stellate cells lacking cGKI could recruit macrophages, which infiltrate the liver promoting inflammatory processes. Elevated inflammation was shown to cause insulin resistance via reduced vascular NO level and

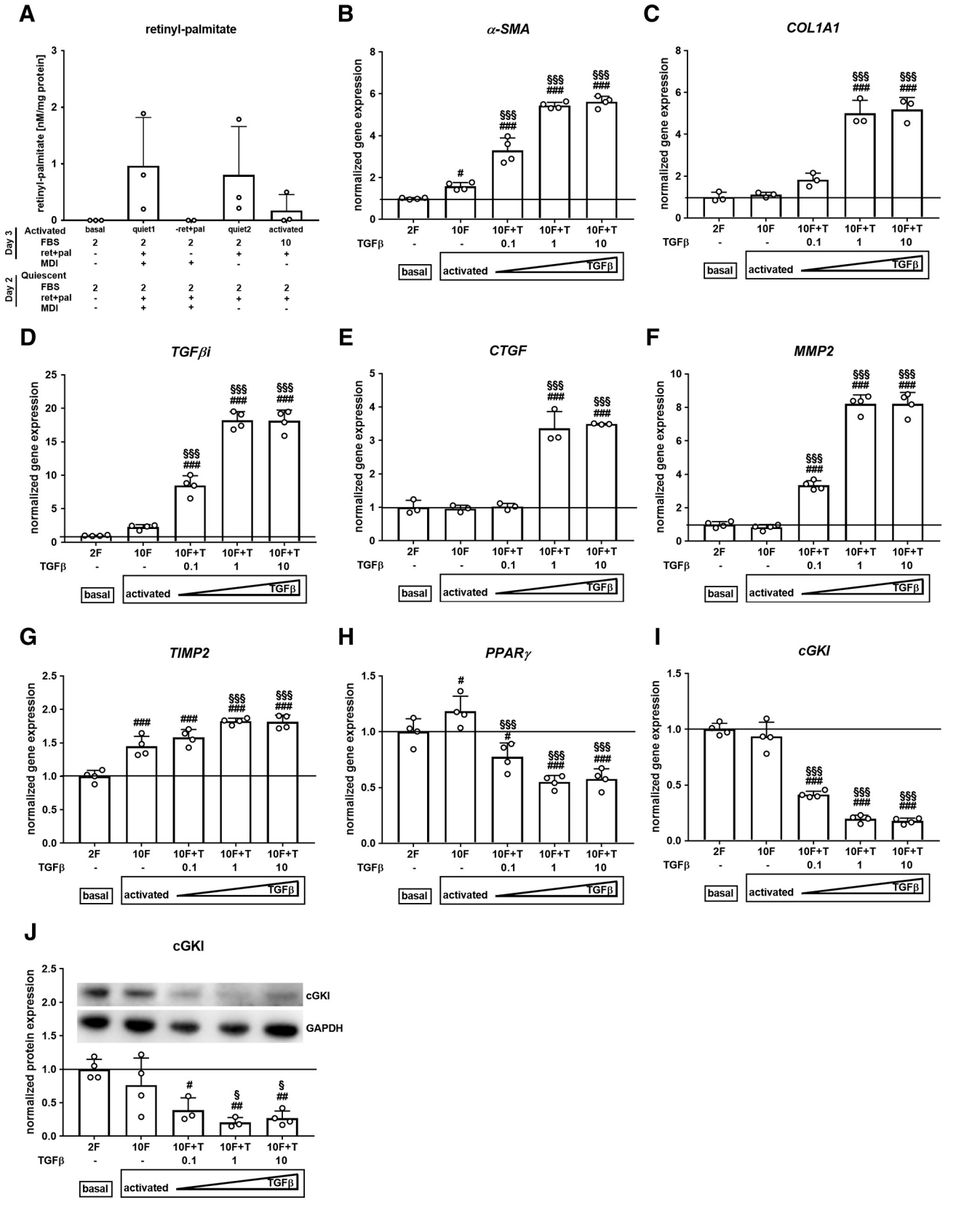

Fig. 2. cGKI level decreases during activation of stellate cells. *A*: Intracellular retinyl-palmitate level was measured by high-performance liquid chromatography. *B–J*: LX2 cells were left untreated in 2% FBS (2F, basal condition) or got activated with 10% FBS (10F) in the presence or absence of 0.1, 1 and 10 ng/ml TGFβ (T) for two days. *B–I*: Transcript levels were determined with real-time PCR. Values were normalized to the geometric mean of housekeeping genes *RPS13* and *UBC* and to 2F condition (set as one). *J*: The protein level of cGKI was determined by Western blot and band intensities of cGKI were normalized to loading control GAPDH by densitometry. Columns represent averages ± standard deviations; n:2–3 for A, n:3–4 for B–J. # denotes significant differences compared to 2F basal condition; #$p < 0.05$, ##$p < 0.01$, ###$p < 0.001$, whereas § denotes significant differences compared to 10F condition; §$p < 0.05$, §§§$p <$ 0.001.

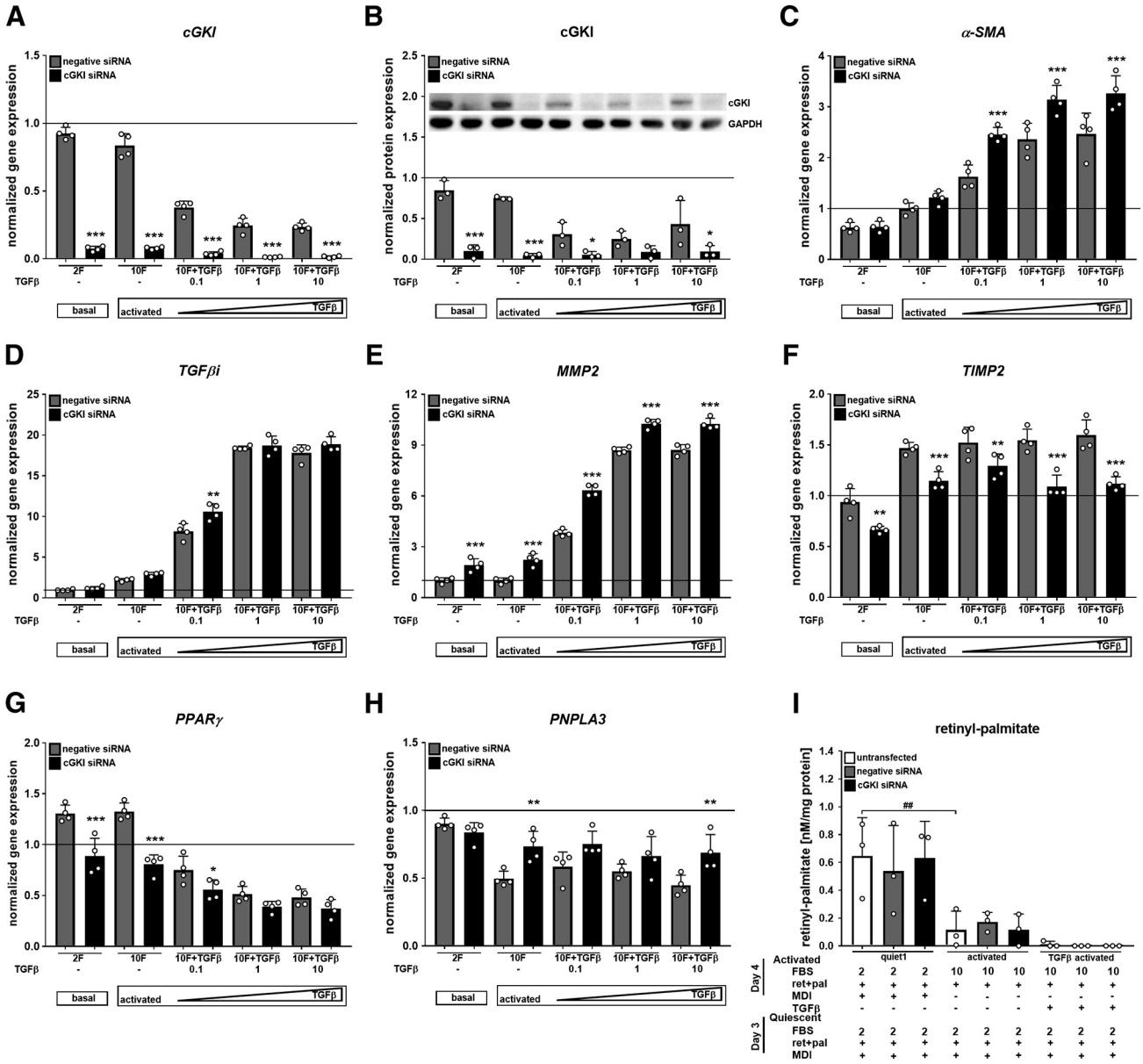

Fig. 3. The ablation of cGKI results in elevated activation of stellate cells. To knock-down cGKI, LX2 cells were transfected with cGKI siRNA or with non-targeting negative control siRNA. *A, C–H*: LX2 cells were left untreated in 2% FBS (2F, basal condition) or got activated with 10% FBS (10F) in the presence or absence of 0.1, 1 and 10 ng/ml TGFβ for two days. Transcript levels were determined with real-time PCR. Values were normalized to the geometric mean of housekeeping genes *RPS13* and *UBC* and to 2F condition of untransfected cells (set as one). *B*: The protein level of cGKI was determined by Western blot and band intensities of cGKI were normalized to loading control GAPDH by densitometry. *I*: Intracellular retinyl-palmitate level was measured by high-performance liquid chromatography. Columns represent averages ± standard deviations; n:3–4. * denotes significant differences between cGKI and negative siRNA control; $^{*}p < 0.05$, $^{**}p < 0.01$, $^{***}p < 0.001$. # denotes significant differences between quiescence condition (quiet1) compared to activated condition for untransfected cells; $\#\#p < 0.01$.

vasodilator-stimulated phosphoprotein (VASP) function, which is a known downstream target of cGKI [35]. Furthermore, a VASP activator displayed protective effects against hepatic inflammation and insulin resistance [35]. Moreover, the activation of cGKI with sildenafil was shown to reduce macrophage infiltration in mouse kidney [28]. These results strongly indicate that the lack of cGKI may play a direct role in recruiting macrophages to the injured liver area and causing hepatic insulin resistance.

The best characterized upstream activator of cGKI is nitric oxide (NO), and a defective NO signaling has been already described in various liver diseases like urea cycle disorders [36], insulin resistance [37], liver fibrosis [38] and cirrhosis [39]. Under physiological conditions, endothelial cells (ECs) keep HSCs via NO signaling quiescent and if the metabolism of EC or HSCs is disturbed, they both could contribute to intrahepatic vascular resistance, which is a characteristic feature of NAFLD [40]. These data underline a contribution of impaired NO/cGMP/cGKI signaling in HSCs to numerous liver diseases.

In our siRNA experiments, silencing cGKI evoked an activated stellate cell profile. Furthermore, cGKI mRNA level was reduced both in activated LX2 stellate cells and in the liver of human subjects with high triacylglycerol (TAG) levels. Thus, these data indicate that hepatic TAG accumulation in human subjects lowers cGKI levels, which in turn could activate stellate cells, promoting hepatic inflammation and in turn insulin resistance.

Animal studies suggested protective effects of cGKI against fibrosis. Overexpression of cGKI or its pharmacological activation was shown to ameliorate kidney fibrosis in mice [28,41]. In rat fibrotic models, liver fibrosis was ameliorated by the application of guanylate-cyclase

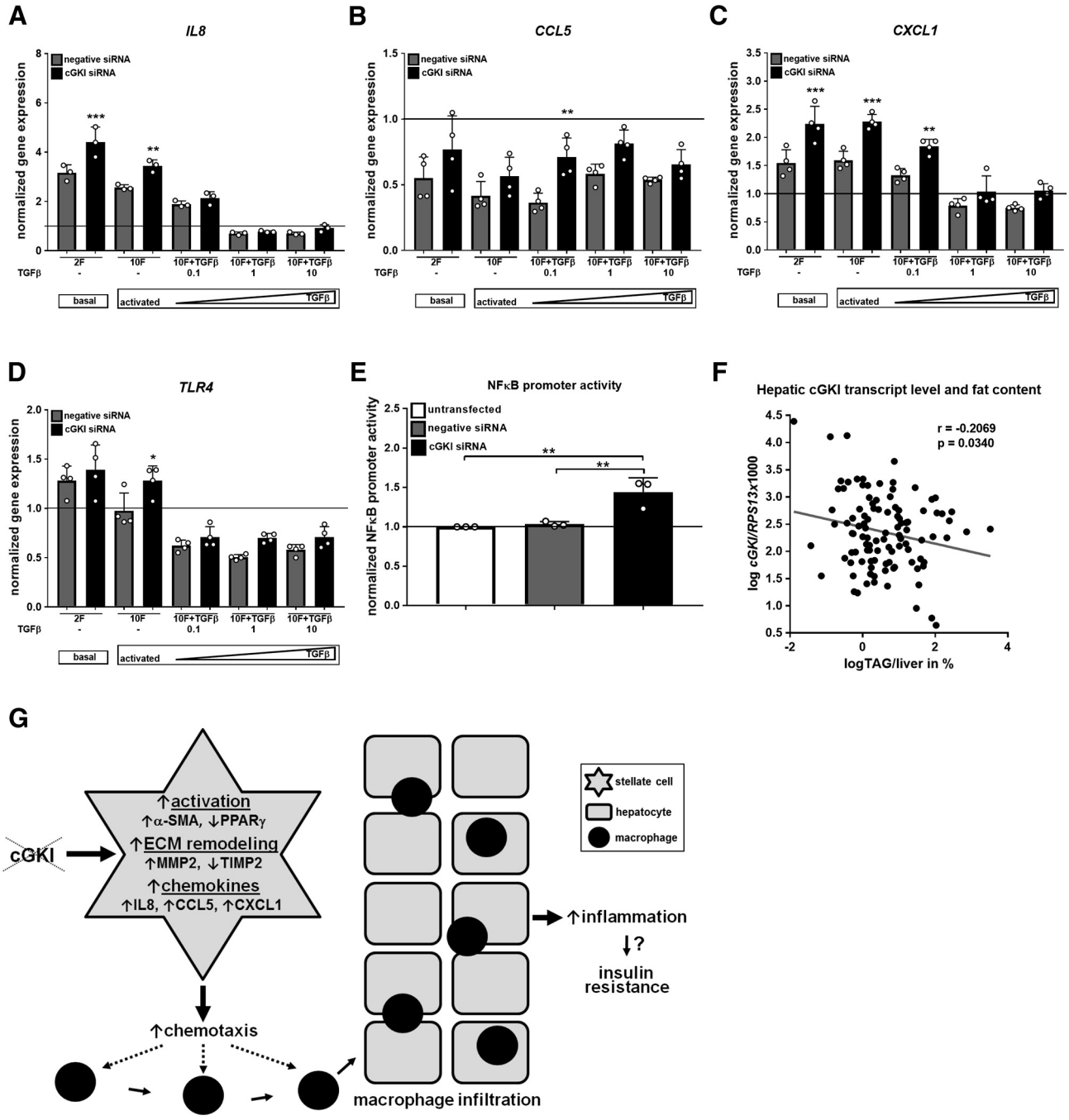

Fig. 4. The ablation of cGKI results in increased chemokine levels and cGKI mRNA levels in human liver biopsies are negatively associated with liver fat. To knock-down cGKI, LX2 cells were transfected with cGKI siRNA or with non-targeting negative control siRNA. *A–D*: LX2 cells were left untreated in 2% FBS (2F, basal condition) or got activated with 10% FBS (10F) in the presence or absence of 0.1, 1 and 10 ng/ml TGFβ. Transcript levels were determined with real-time PCR. Values were normalized to the geometric mean of housekeeping genes *RPS13* and *UBC* and to 2F condition of untransfected cells (set as one). *E*: NFkB promoter activity measured by luciferase assay, which was performed in LX2 cells in the presence of 2% FBS. Columns represent averages ± standard deviations; n:3–4. * denotes significant differences between cGKI and negative siRNA control; $^{*}p < 0.05$, $^{**}p < 0.01$, $^{***}p < 0.001$. *F*: Correlation between the hepatic expression of cGKI and liver fat in human subjects. In human liver biopsies, cGKI mRNA level was determined with real-time PCR and values were normalized to the housekeeping gene *RPS13* expression. Liver fat content was measured by clinical chemistry. Linear correlation was calculated on logarithmic transformed data; n:105. *G*: Putative molecular mechanisms describing the link between the ablation of cGKI and hepatic insulin resistance. Our data suggest that cGKI modulates at least three major functions of stellate cells (for details, see Section 4). **Function 1**: The lack of cGKI increased transcript level of *α-SMA* and decreased mRNA level of *PPARγ*, which could result in higher activation state of LX2 cells. **Function 2**: The ablation of cGKI elevated transcript level of *MMP2* and reduced mRNA level of *TIMP2*, which could lead to an altered matrix remodeling activity. **Function 3**: The absence of cGKI induced the transcript levels of *IL8*, *CCL5* and *CXCL1*. Chemokines could recruit macrophages, which infiltrate the liver and induce inflammatory processes, which in turn may lead to insulin resistance.

activator BAY 60-2770, which increases cGMP level and possibly activates cGKI [42]. Furthermore in mice, skin fibrosis was also improved in a cGKI-dependent manner [43]. These results implicate, that drugs elevating cGKI activity may be promising targets protecting from fibrosis.

In conclusion, our data provide new evidence, that cGKI regulates hepatic stellate cell activation. Giving that downregulation of this pathway could promote inflammatory processes and insulin resistance, our results provide the basis for future investigations at modifying treatment in patients with liver steatosis and/or fibrosis.

Supplementary data to this article can be found online at https://doi.org/10.1016/j.metabol.2018.09.001.

Author Contributions

A.F. and S.Z.L. conceived the experiments, researched the data, revised and approved the manuscript. M.K. and M.R. researched the data, revised and approved the manuscript. R.W., M.H., A.K. and A.K.N. provided material, revised and approved the manuscript. S.F., R.F., C.W., H.U.H. and A.P. conceived the experiments, revised and approved the manuscript. A.F. and A.P. wrote the manuscript.

Funding

This work was supported by a grant from the German Federal Ministry of Education and Research (BMBF) to the German Center for Diabetes Research (DZD e.V.).

Conflict of Interests

None.

Acknowledgments

We thank Alke Guirguis, Nadine Vilas and Dorothee Neuscheler (Department of Internal Medicine IV, Division of Endocrinology, Diabetology, Angiology, Nephrology and Clinical Chemistry, University Hospital Tübingen, Tübingen, Germany) for excellent technical assistance. We also gratefully acknowledge Dr. Benjamin A. Jaghutriz, Ines Wagener, Andreas Vosseler, Anja Dessecker and Ellen Kollmar for their assistance in the clinical studies (Department of Internal Medicine IV, Division of Endocrinology, Diabetology, Angiology, Nephrology and Clinical Chemistry, University Hospital Tübingen, Tübingen, Germany). We thank Jakob Matthes (c.ATG Medical Genetics and Applied Genomics, Tübingen, Germany) for the microarray analysis.

References

[1] Stefan N, Schick F, Haring HU. Causes, characteristics, and consequences of metabolically unhealthy normal weight in humans. Cell Metab 2017;26:292–300.
[2] Stefan N, Haring HU. The role of hepatokines in metabolism. Nat Rev Endocrinol 2013;9:144–52.
[3] Tsuchida T, Friedman SL. Mechanisms of hepatic stellate cell activation. Nat Rev Gastroenterol Hepatol 2017;14:397–411.
[4] Weiskirchen R, Tacke F. Cellular and molecular functions of hepatic stellate cells in inflammatory responses and liver immunology. Hepatobiliary Surg Nutr 2014;3:344–63.
[5] Palladini G, Ferrigno A, Richelmi P, Perlini S, Vairetti M. Role of matrix metalloproteinases in cholestasis and hepatic ischemia/reperfusion injury: a review. World J Gastroenterol 2015;21:12114–24.
[6] Lee YA, Wallace MC, Friedman SL. Pathobiology of liver fibrosis: a translational success story. Gut 2015;64:830–41.
[7] Karagozian R, Derdak Z, Baffy G. Obesity-associated mechanisms of hepatocarcinogenesis. Metabolism 2014;63:607–17.
[8] Peters KM, Wilson RB, Borradaile NM. Non-parenchymal hepatic cell lipotoxicity and the coordinated progression of non-alcoholic fatty liver disease and atherosclerosis. Curr Opin Lipidol 2018;29:417–22.
[9] Lutz SZ, Hennige AM, Feil S, Peter A, Gerling A, Machann J, et al. Genetic ablation of cGMP-dependent protein kinase type I causes liver inflammation and fasting hyperglycemia. Diabetes 2011;60:1566–76.
[10] Schlossmann J, Feil R, Hofmann F. Insights into cGMP signalling derived from cGMP kinase knockout mice. Front Biosci 2005;10:1279–89.
[11] Baffy G. Origins of portal hypertension in nonalcoholic fatty liver disease. Dig Dis Sci 2018;63:563–76.
[12] Balletshofer BM, Rittig K, Enderle MD, Volk A, Maerker E, Jacob S, et al. Endothelial dysfunction is detectable in young normotensive first-degree relatives of subjects with type 2 diabetes in association with insulin resistance. Circulation 2000;101:1780–4.
[13] Xu L, Hui AY, Albanis E, Arthur MJ, O'Byrne SM, Blaner WS, et al. Human hepatic stellate cell lines, LX-1 and LX-2: new tools for analysis of hepatic fibrosis. Gut 2005;54:142–51.
[14] Weber S, Bernhard D, Lukowski R, Weinmeister P, Worner R, Wegener JW, et al. Rescue of cGMP kinase I knockout mice by smooth muscle specific expression of either isozyme. Circ Res 2007;101:1096–103.
[15] Franko A, Neschen S, Rozman J, Rathkolb B, Aichler M, Feuchtinger A, et al. Bezafibrate ameliorates diabetes via reduced steatosis and improved hepatic insulin sensitivity in diabetic TallyHo mice. Mol Metab 2017;6:256–66.
[16] Kovarova M, Konigsrainer I, Konigsrainer A, Machicao F, Haring HU, Schleicher E, et al. The genetic variant I148M in PNPLA3 is associated with increased hepatic Retinyl-palmitate storage in humans. J Clin Endocrinol Metab 2015;100:E1568–74.
[17] Franko A, Huypens P, Neschen S, Irmler M, Rozman J, Rathkolb B, et al. Bezafibrate improves insulin sensitivity and metabolic flexibility in STZ-induced diabetic mice. Diabetes 2016;65:2540–52.
[18] Knobeloch D, Ehnert S, Schyschka L, Buchler P, Schoenberg M, Kleeff J, et al. Human hepatocytes: isolation, culture, and quality procedures. Methods Mol Biol 2012;806:99–120.
[19] Wu Y, Liu X, Zhou Q, Huang C, Meng X, Xu F, et al. Silent information regulator 1 (SIRT1) ameliorates liver fibrosis via promoting activated stellate cell apoptosis and reversion. Toxicol Appl Pharmacol 2015;289:163–76.
[20] Pingitore P, Dongiovanni P, Motta BM, Meroni M, Lepore SM, Mancina RM, et al. PNPLA3 overexpression results in reduction of proteins predisposing to fibrosis. Hum Mol Genet 2016;25:5212–22.
[21] Peter A, Kantartzis K, Machicao F, Machann J, Wagner S, Templin S, et al. Visceral obesity modulates the impact of apolipoprotein C3 gene variants on liver fat content. Int J Obes 2012;36:774–82.
[22] Hoffmann C, Hockele S, Kappler L, Hrabe de Angelis M, Haring HU, Weigert C. The effect of differentiation and TGFbeta on mitochondrial respiration and mitochondrial enzyme abundance in cultured primary human skeletal muscle cells. Sci Rep 2018;8:737.
[23] Burt D, Brodbeck K, Haring HU, Schleicher ED, Weigert C. Partial characterisation of the human GFAT promoter: effect of single nucleotide polymorphisms on promoter function. Biochim Biophys Acta 1740;2005:85–90.
[24] Schon HT, Weiskirchen R. Immunomodulatory effects of transforming growth factor-beta in the liver. Hepatobiliary Surg Nutr 2014;3:386–406.
[25] Robert S, Gicquel T, Bodin A, Lagente V, Boichot E. Characterization of the MMP/TIMP imbalance and collagen production induced by IL-1beta or TNF-alpha release from human hepatic stellate cells. PLoS One 2016;11:e0153118.
[26] Koyama Y, Brenner DA. Liver inflammation and fibrosis. J Clin Invest 2017;127:55–64.
[27] Iredale JP. Models of liver fibrosis: exploring the dynamic nature of inflammation and repair in a solid organ. J Clin Invest 2007;117:539–48.
[28] Cui W, Maimaitiyiming H, Qi X, Norman H, Zhou Q, Wang X, et al. Increasing cGMP-dependent protein kinase activity attenuates unilateral ureteral obstruction-induced renal fibrosis. Am J Physiol Ren Physiol 2014;306:F996–F1007.
[29] Mann J, Chu DC, Maxwell A, Oakley F, Zhu NL, Tsukamoto H, et al. MeCP2 controls an epigenetic pathway that promotes myofibroblast transdifferentiation and fibrosis. Gastroenterology 2010;138:705–14 [14.e1–4].
[30] Bourboulia D, Stetler-Stevenson WG. Matrix metalloproteinases (MMPs) and tissue inhibitors of metalloproteinases (TIMPs): positive and negative regulators in tumor cell adhesion. Semin Cancer Biol 2010;20:161–8.
[31] Iredale JP. Hepatic stellate cell behavior during resolution of liver injury. Semin Liver Dis 2001;21:427–36.
[32] Fujita T, Narumiya S. Roles of hepatic stellate cells in liver inflammation: a new perspective. Inflamm Regen 2016;36:1.
[33] Pozniak KN, Pearen MA, Pereira TN, Kramer CSM, Kalita-De Croft P, Nawaratna SK, et al. Taurocholate induces biliary differentiation of liver progenitor cells causing hepatic stellate cell chemotaxis in the ductular reaction: role in pediatric cystic fibrosis liver disease. Am J Pathol 2017;187:2744–57.
[34] Clement S, Pascarella S, Conzelmann S, Gonelle-Gispert C, Guilloux K, Negro F. The hepatitis C virus core protein indirectly induces alpha-smooth muscle actin expression in hepatic stellate cells via interleukin-8. J Hepatol 2010;52:635–43.
[35] Kang YM, Kim F, Lee WJ. Role of NO/VASP signaling pathway against obesity-related inflammation and insulin resistance. Diabetes Metab J 2017;41:89–95.
[36] Nagasaka H, Tsukahara H, Yorifuji T, Miida T, Murayama K, Tsuruoka T, et al. Evaluation of endogenous nitric oxide synthesis in congenital urea cycle enzyme defects. Metabolism 2009;58:278–82.
[37] Artunc F, Schleicher E, Weigert C, Fritsche A, Stefan N, Haring HU. The impact of insulin resistance on the kidney and vasculature. Nat Rev Nephrol 2016;12:721–37.
[38] Poisson J, Lemoinne S, Boulanger C, Durand F, Moreau R, Valla D, et al. Liver sinusoidal endothelial cells: physiology and role in liver diseases. J Hepatol 2017;66:212–27.
[39] Loureiro-Silva MR, Iwakiri Y, Abraldes JG, Haq O, Groszmann RJ. Increased phosphodiesterase-5 expression is involved in the decreased vasodilator response to nitric oxide in cirrhotic rat livers. J Hepatol 2006;44:886–93.
[40] Deleve LD, Wang X, Guo Y. Sinusoidal endothelial cells prevent rat stellate cell activation and promote reversion to quiescence. Hepatology 2008;48:920–30.
[41] Schinner E, Schramm A, Kees F, Hofmann F, Schlossmann J. The cyclic GMP-dependent protein kinase Ialpha suppresses kidney fibrosis. Kidney Int 2013;84:1198–206.
[42] Knorr A, Hirth-Dietrich C, Alonso-Alija C, Harter M, Hahn M, Keim Y, et al. Nitric oxide-independent activation of soluble guanylate cyclase by BAY 60-2770 in experimental liver fibrosis. Arzneimittelforschung 2008;58:71–80.
[43] Matei AE, Beyer C, Gyorfi AH, Soare A, Chen CW, Dees C, et al. Protein kinases G are essential downstream mediators of the antifibrotic effects of sGC stimulators. Ann Rheum Dis 2018;77:459.